JOURNAL OF CIVIL ENGINEERING PLANNING and DESIGN

*Journal of Civil Engineering, Planning, and Design Vol. 2, No. 1, 2023: page 14-20*



# Stress Analysis of PCI-Girder Precast Concrete Segmental Bridge Based on SNI 1725:2016 (Case Study: Konaweha River Bridges, Southeast Sulawesi)

Nia Dwi Puspitasari[1a1], Wahyu Kartini[2a], Achmad Dzulfiqar Alfiansyah[3a]

[a] *Department of Civil Engineering, Engineering Faculty, UPN "Veteran" East Java, Surabaya 60294, Indonesia*

**Abstract**. A prestressed bridge is an alternative way of structural design because of the ease of procurement and installation. For long-span bridges, prestressed beams only require minimum cross-sectional dimensions along with reliable performance. A prestressed concrete beam is always made in several segments to facilitate delivery. It is necessary to analyse and control the stress that occurs due to the external load and the loss of prestress. This study aims to provide a detailed stress analysis of PCI-girder precast concrete segmental bridges, considering the provisions and guidelines specified in SNI 1725:2016. Four stages of construction will be controlled. Namely at the transfer stage, the after-loss of the prestressed stage, the composite beam stage, and the service stage. The tensile and compressive stress analyses will be carried out on the upper side of the bridge surface, the upper side of the girder, and the bottom. If tensile stress occurs, it indicates that the girder is not capable of withstanding the applied load, and additional anchorages need to be installed at each joint between segments. The result obtained from the stress analysis conducted in this study is that no tensile stress is found in any critical sections of the girder. The stress that occurs has fulfilled the design capacity, without any tensile stress occurring in the bridge.

***Keywords:*** Compressive stress, Prestressed concrete, Segmental girders, Tensile stress

## 1. Introduction

Precast concrete has become the most favoured alternative for bridge construction due to its economic value, speed and ease of construction, and minimal impact on the environment. Internal prestressed tendons are used to enhance the ductility of concrete, while external tendons are employed for maintenance and to anticipate construction activities when additional tensile forces are required [1]–[3]. PCI Girder is a type of precast concrete beam that is often used in bridge construction. To facilitate delivery, PCI Girder is produced in several segments. Konaweha is the location or project where the PCI Girder is installed on the bridge. Analysis of the stress value on the Konaweha Bridge Girder PCI is important to ensure the safety and reliability of the bridge, especially at the joints between segments.

It is crucial to prevent any tensile stress from occurring on the segmental bridge as it can lead to structural damage and pose a risk to the safety of bridge users. The overall stiffness and stability of the girder decrease as the number of segments increases [4]–[6]. The stress to be analysed is at the top and bottom sides of the bridge because it is at this position that the maximum stress occurs. This study aims to provide a detailed stress analysis of PCI-girder precast concrete segmental bridges, considering the provisions and guidelines specified in SNI 1725:2016 [7].
To achieve this objective, the research methodology involves a systematic approach that encompasses stress analysis at transfer conditions, after the loss of prestress, at the composite beam stage, and the service stage. The study focuses on the key aspects of stress analysis, including but not limited to, the evaluation of dead loads, live loads, environmental loads, and prestress forces acting on the bridge.

By investigating the stress distribution, load effects, and performance indicators, valuable insights can be gained to enhance the design and construction practices of such bridges. If tensile stresses are found on the bridge, anchoring the segments between the bridges is necessary. Additionally, the study will provide valuable recommendations and insights for bridge engineers, designers, and researchers involved in the design, analysis, and construction of similar bridge structures.
In conclusion, this article presents an in-depth analysis of stress factors and load effects on PCI-girder precast concrete segmental bridges based on the SNI 1725:2016 standard. The research findings will contribute to the advancement of knowledge in this field, ultimately enhancing the safety and efficiency of precast concrete segmental bridge designs in Indonesia.

## 2. Methods

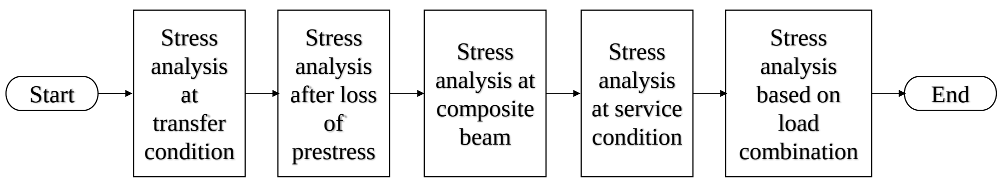


**Fig. 1** Flow chart of the research methodology

### *2.1 Bridges Specification*

The bridge has a PC-I Girder with a span ($L$) of 40,8 m and a cross-sectional area ($A$) of 0,753 m$^3$. The moment resistance at the upper side ($W_a$) is 0,378 m$^3$, and the bottom side ($W_a$) is 0,410 m$^3$. The total prestressing load ($P_t$) of 64 prestressing steel obtained a total load value of 9053 kN. The concrete strength at 28 days after production ($f'_c$) is 41.500 kPa with the allowable compressive

[1] Corresponding author: nia.dwi.ts@upnjatim.ac.id

stress being 0,45 of $f'_c$ or about 18.675 kPa. The eccentricity value of the prestressing steel in the mid-span is 210 and 100 cm based on Fig. 1.

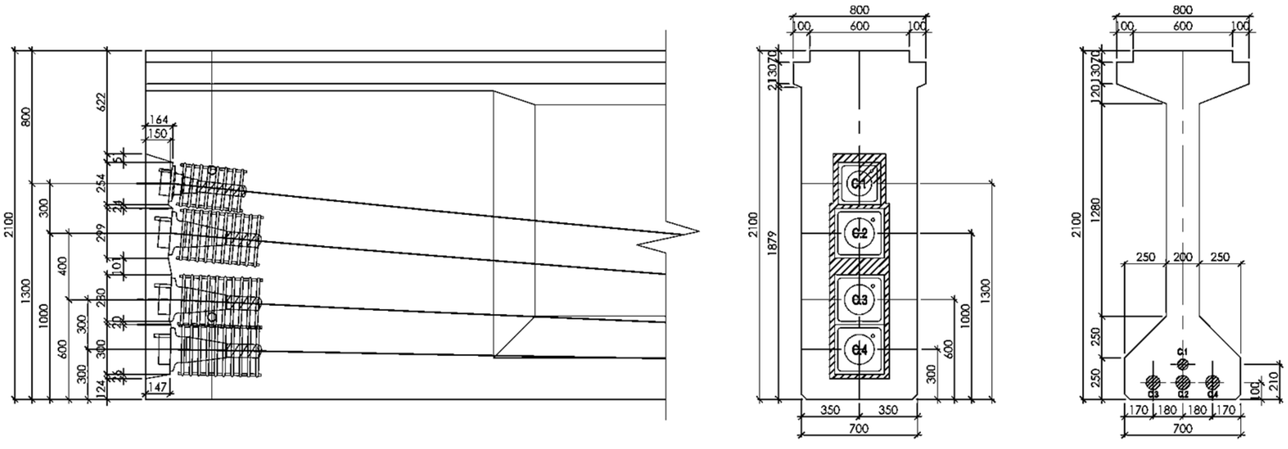


**Fig. 2** Prestressing steel configuration and cross-section of the beam.

*2.2 Load Analysis*

Based on the provided cross-sectional data and by the loading regulations specified in SNI 1725:2016, the magnitude of the loads occurring on the bridge can be summarized in the following table: Table 1.

**Table 1**
Loads summary on prestressed beams

| | Load | Symbol | Uniformly distributed load (q) kN/m | Fixed Load (P) kN | Moment (M) kN.m |
|---|---|---|---|---|---|
| 1. | Self-weight Load | MS | 36,94 | - | - |
| 2. | Additional Dead Load | MA | 4,98 | - | - |
| 3. | "D" Line Load | TD | 12,84 | 113,96 | - |
| 4. | Braking Load | TB | - | - | 155,22 |
| 5. | Wind Load | EW | 1,01 | - | - |
| 6. | Earthquake Load | EQ | 4,19 | - | - |

The specific values for each load type will be determined based on the cross-sectional data and the corresponding provisions of SNI 1725:2016. These load values are crucial for conducting a comprehensive analysis of the bridge's structural behavior and ensuring its safe and efficient performance under various loading conditions. The maximum shear force and bending moment that occur on the bridge due to the variation and types of loads mentioned in Table 1 also can be obtained. The results of the shear force diagram and moment diagram have been presented in previous research [8].

*2.3 Stress analysis at transfer condition*

The transfer Stage is when the prestressing force is applied to the beam during the installation stage [9]. There are only consist of the prestressing force and the self-weight load. At this stage, the quality of the concrete has not been fully accomplished but already meets the requirements. When the concrete is still at initial condition ($f_{ci}$) or 0.8 $f'_c$ (based on SNI) with the value of 33.200 kPa. With $f'_c$ it indicates the concrete strength at 28 days after production. The stress value at the top and the bottom of the beam can be obtained from the following equation:

$$f_{ca} = -\frac{P_t}{A} + \frac{P_t \cdot e_s}{W_a} - \frac{M_{beam}}{W_a} \quad (1)$$

$$f_{cb} = -\frac{P_t}{A} - \frac{P_t \cdot e_s}{W_b} + \frac{M_{beam}}{W_b} \quad (2)$$

The stress value at the upper side of the beam ($f_{ca}$) is -3.451 kPa (compression) and the stress value at the bottom side of the beam ($f_{cb}$) is -19.820 kPa (compression). There is a larger compression stress value occurs at the bottom side of the beam. This indicates that upward deflection occurs during the transfer stage. The allowable compressive stress at the initial condition value is 0,6 $f'_{ci}$ or about 19.920 kPa. It can be concluded that the stress value that occurs at the upper and the bottom side of the beam is still under the allowable compressive stress at the initial condition.

*2.4 Stress analysis after the loss of prestress*

At this point, the concrete strength has reached its optimal state and is displayed as $f'_c$. The prestressing load immediately after installing the segmental girder is reduced by about 30% of the total prestressing load ($P_t$). The reduction in prestressing load due to loss of prestressed is indicated by $P_{eff}$. The cross-sectional shape remains the same as the PC-I beam, so the values of $W_a$,

$W_b$, and $A$ remain the same as the transfer conditions. The stress value at the top and the bottom of the beam at this stage can be obtained from the following equation:

$$f_a = -\frac{P_{eff}}{A} + \frac{P_{eff} \cdot e_s}{W_a} - \frac{M_{beam}}{W_a} \quad (3)$$

$$f_b = -\frac{P_{eff}}{A} - \frac{P_{eff} \cdot e_s}{W_b} + \frac{M_{beam}}{W_b} \quad (4)$$

The stress value at the upper side of the beam ($f_a$) is -4.601 kPa (compression) and the stress value at the bottom side of the beam ($f_b$) is -15.853 kPa (compression). There is a larger compression stress value occurs at the bottom side of the beam. This indicates that upward deflection occurs after the loss of prestress. The allowable compressive stress after the loss of prestress is 0,45 $f'_c$ or about 18.675 kPa. It can be concluded that the stress value that occurs at the upper and the bottom side of the beam is still under the allowable compressive stress after the loss of prestress.

*2.5 Stress analysis at composite beam*

At this stage, the concrete strength is denoted by $f'_c$ and the prestress load is denoted by $P_{eff}$ as it occurs after the prestress is lost. Since the deck is installed on top of the girder, the cross-sectional shape changes to a T-shape. Using this T shape as a reference, the values of the upper moment resistance of the beam and slab ($W_{ac}$), the lower side moment resistance of the beam and slab ($W_{bc}$), and the beam and slab cross-sectional area ($A_c$) can be found. The stress value can be obtained from the following equation:

$$f_{ac} = -\frac{P_{eff}}{A_c} + \frac{P_{eff} \cdot e_s}{W_{ac}} - \frac{M_{beam+slab}}{W_{ac}} \quad (5)$$

$$f_{bc} = -\frac{P_{eff}}{A_c} - \frac{P_{eff} \cdot e_s}{W_{bc}} + \frac{M_{beam+slab}}{W_{bc}} \quad (6)$$

The stress value at the upper side of the slab ($f_{ac}$) is -4.110 kPa (compression). The intersection between the slab and the girder ($f'_{ac}$) has a stress value of -4.870 kPa (compression). The stress value at the bottom side of the girder ($f_{bc}$) is -12.854 kPa (compression). There is a larger compression stress value occurs at the bottom side of the beam. This indicates that upward deflection still occurs during the composite beam stage. The allowable compressive stress at the composite beam stage is 0,45 $f'_c$ or about 18.675 kPa. It can be concluded that the stress value that occurs at the upper and the bottom side of the beam is still under the allowable compressive stress in the composite beam stage.

*2.6 Stress analysis at service condition*

There are three groups of loads that occur on the bridge at service conditions. These loads include, firstly, the fixed load, which is caused by a constant load experienced by the bridge and does not change over time. Secondly, there is the transient load, which is a result of traffic loads from vehicles and varies in magnitude depending on the vehicles passing over the bridge. The third load is the environmental load, which is a result of changes in the environment that ultimately affect the condition of the bridge [10].

*2.6.1 Fixed load*

The fixed load is a load that does not change over time and consists of four types of loads: self-weight load, additional dead load, shrinkage load, and prestressing force. The stress value caused by each of these loads will be explained as follows:

- Self-weight load and additional dead load

  The stress value at the top ($f_{ac}$) and the bottom of the beam ($f_{bc}$) can be obtained from the following equation:

$$f_{ac} = -\frac{M_S}{W_{ac}} \quad (7)$$

$$f_{bc} = +\frac{M_S}{W_{bc}} \quad (8)$$

  With $M_s$ representing the value of the moment caused by the self-weight load (*MS*) and additional dead load (*MA*), as summarized in Table 1. Since the bridge is a simple beam, the value of the moment can be determined using the following formula:

$$M_s = \frac{1}{8} \cdot q \cdot L^2 \quad (9)$$

  The stress value due to the self-weight at the upper side of the slab ($f_{ac}$) is -11.482 kPa (compression). The intersection between the slab and the girder ($f'_{ac}$) has a stress value of -9.196 kPa (compression). The stress value at the bottom side of the girder ($f_{bc}$) is +14.810 kPa (tension). The stress value due to the additional dead load at the upper side of the slab ($f_{ac}$) is -1.547 kPa (compression). The intersection between the slab and the girder ($f'_{ac}$) has a stress value of -1.239 kPa (compression). The stress

JCEPD-ISSN: 2830-3628

value at the bottom side of the girder ($f_{bc}$) is +1.995 kPa (tension). These stresses will then be combined with other loads to obtain the stress behavior that represents the actual loading conditions occurring on the bridge.

- Shrinkage load

Shrinkage load refers to the internal stresses and deformations that occur in a structure due to the drying and shrinking of concrete over time. Concrete tends to undergo volume reduction as it cures and loses moisture, leading to shrinkage. This shrinkage can exert forces on the structure, resulting in additional loads known as shrinkage loads. These loads can contribute to the overall stress and deformation of the bridge [11]. The stress value at the top ($f_{ac}$) and the bottom of the beam ($f_{bc}$) due to shrinkage load can be obtained from the following equation:

$$f_{ac} = +\frac{P_s}{A_c} - \frac{P_s \cdot e'}{W_{ac}} \quad (10)$$

$$f_{bc} = +\frac{P_s}{A_c} + \frac{P_s \cdot e'}{W_{bc}} \quad (11)$$

With e′ represents the eccentricity or the distance between the centroid of the slab and the centroid of the beam. An illustration of the position of e′ can be seen in Fig. 1. While $P_s$ represents the magnitude of the shrinkage load experienced by the bridge slab.

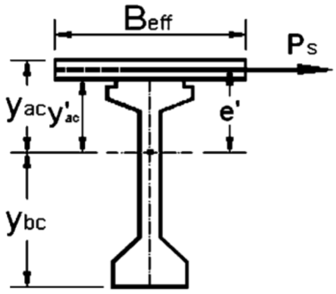


**Fig. 3** Illustration of the position of e′ on the bridge.

The stress value due to the shrinkage load at the upper side of the slab ($f_{ac}$) is -945 kPa (compression). The intersection between the slab and the girder ($f'_{ac}$) has a stress value of -441 kPa (compression). The stress value at the bottom side of the girder ($f_{bc}$) is -804 kPa (compression). These stresses will then be combined with other loads to obtain the stress behavior that represents the actual loading conditions occurring on the bridge.

- Prestressing force

The prestressing force at service conditions is lower than the initial prestressing force due to the loss of prestress. Estimating the loss of prestress at the planning and design stage is essential. After subtracting the prestress losses, the remaining prestressing force, denoted by $P_{eff}$, in the prestressing tendon is still sufficient to provide the necessary concrete stress to withstand the applied service loads [12]. The remaining prestressing force after being reduced by the loss of prestressing is denoted by $P_{eff}$. The stress value at the top ($f_{ac}$) and the bottom of the beam ($f_{bc}$) due to prestressing force can be obtained from the following equation:

$$f_{ac} = -\frac{P_{eff}}{A_c} + \frac{P_{eff} \cdot e'_s}{W_{ac}} \quad (12)$$

$$f_{bc} = -\frac{P_{eff}}{A_c} - \frac{P_{eff} \cdot e'_s}{W_{bc}} \quad (13)$$

With the value of $P_{eff}$ being 7.875 kN or having undergone a 30% reduction, the stress value at the upper side of the slab ($f_{ac}$) is +5.695 kPa (tension). The intersection between the slab and the girder ($f'_{ac}$) has a stress value of +2.983 kPa (tension). The stress value at the bottom side of the girder ($f_{bc}$) is -25.502 kPa (compression). These stresses will then be combined with other loads to obtain the stress behavior that represents the actual loading conditions occurring on the bridge.

2.6.2 Transient Load

Transient load is the load resulting from a vehicle passing over the bridge. Two types of loads are classified as transient loads: the "D" lane load and the braking load. The stress value at the top ($f_{ac}$) and the bottom of the beam ($f_{bc}$) due to transient load can be obtained from the following equation:

$$f_{ac} = -\frac{M_T}{W_{ac}} \quad (14)$$

$$f_{bc} = +\frac{M_T}{W_{bc}} \quad (15)$$

$M_T$ represents the magnitude of the moment caused by the "D" lane load, whether it is a Uniform Distributed Load (UDL) or a Knife Edge Load (KEL), as stated in Table 1. Equation (9) can be used to calculate the moment due to UDL. And the following equation can be used to obtain the moment value due to KEL:

$$M_T = \frac{1}{4} \cdot P \cdot L \quad (16)$$

As for the braking load, it can be directly substituted into equation (14) or equation (15) since the braking load already results in a specific moment value. The stress value caused by the "D" lane load at the upper side of the slab ($f_{ac}$) is -5.728 kPa (compression). The intersection between the slab and the girder ($f'_{ac}$) has a stress value of -4.588 kPa (compression). The stress value at the bottom side of the girder ($f_{bc}$) is +7.388 kPa (tension). The stress value due to the braking load at the upper side of the slab ($f_{ac}$) is -116 kPa (compression). The intersection between the slab and the girder ($f'_{ac}$) has a stress value of -93 kPa (compression). The stress value at the bottom side of the girder ($f_{bc}$) is +150 kPa (tension). These stresses will then be combined with other loads to obtain the stress behavior that represents the actual loading conditions occurring on the bridge.

2.6.3 Environmental load

Environmental load is the load resulting from environmental influences, consisting of temperature load, wind load, and earthquake load [13]. The stress value at the top ($f_{ac}$) and the bottom of the beam ($f_{bc}$) due to environmental load can be obtained from the following equation:

$$f_{ac} = -\frac{M_E}{W_{ac}} \quad (17)$$

$$f_{bc} = +\frac{M_E}{W_{bc}} \quad (18)$$

$M_E$ represents the magnitude of the moment caused by the wind load and earthquake load as stated in Table 1. Equation (9) can be used to calculate the moment due to both wind load and earthquake load. The stress value caused by the temperature load at the upper side of the slab ($f_{ac}$) is -1.532 kPa (compression). The intersection between the slab and the girder ($f'_{ac}$) has a stress value of -1.990 kPa (compression). The stress value at the bottom side of the girder ($f_{bc}$) is -912 kPa (compression). The stress value due to wind load at the upper side of the slab ($f_{ac}$) is -313 kPa (compression). The intersection between the slab and the girder ($f'_{ac}$) has a stress value of -251 kPa (compression). The stress value at the bottom side of the girder ($f_{bc}$) is +404 kPa (tension). The stress value due to earthquake load at the upper side of the slab ($f_{ac}$) is -1.303 kPa (compression). The intersection between the slab and the girder ($f'_{ac}$) has a stress value of -1.044 kPa (compression). The stress value at the bottom side of the girder ($f_{bc}$) is +1.681 kPa (tension). These stresses will then be combined with other loads to obtain the stress behavior that represents the actual loading conditions occurring on the bridge.

## 3. Result and Discussion

Based on the calculation analysis as described in the methodology section above, the results obtained are summarized in Table 2 and Table 3.

**Table 2**

Stress analysis results based on combination 1, combination 2, and combination 3

| Load | Stress Value of Each Combination (kPa) | | | | | | | | |
|---|---|---|---|---|---|---|---|---|---|
| | Combination 1 | | | Combination 2 | | | Combination 3 | | |
| | $f_{ac}$ | $f'_{ac}$ | $f_{bc}$ | $f_{ac}$ | $f'_{ac}$ | $f_{bc}$ | $f_{ac}$ | $f'_{ac}$ | $f_{bc}$ |
| **A. Fixed Load** | | | | | | | | | |
| 1. Self-weight Load | -11482 | -9196 | 14810 | -11482 | -9196 | 14810 | -11482 | -9196 | 14810 |
| 2. Additional Dead Load | -1547 | -1239 | 1995 | -1547 | -1239 | 1995 | -1547 | -1239 | 1995 |
| 3. Shrinkage | -945 | -411 | -804 | -945 | -411 | -804 | -945 | -411 | -804 |
| 4. Prestressing Force | 5695 | 2983 | -25502 | 5695 | 2983 | -25502 | 5695 | 2983 | -25502 |
| **B. Transient Load** | | | | | | | | | |
| 1. "D" Line Load | -5728 | -4588 | 7388 | -5728 | -4588 | 7388 | -5728 | -4588 | 7388 |
| 2. Brakingbr Load | -116 | -93 | 150 | -116 | -93 | 150 | -116 | -93 | 150 |
| **C. Environment Load** | | | | | | | | | |
| 1. Temperature | - | - | - | -1532 | -1990 | -912 | - | - | - |
| 2. Wind Load | - | - | - | - | - | - | -313 | -251 | 404 |
| 3. Earthquake Load | - | - | - | - | - | - | - | - | - |
| **Stress Result** | **-14123** | **-12544** | **-1963** | **-15655** | **-14534** | **-2875** | **-14437** | **-12795** | **-1559** |

JCEPD-ISSN: 2830-3628

**Table 3**
Stress analysis results based on combination 4, and combination 5

| Load | Stress Value of Each Combination (kPa) | | | | | |
|---|---|---|---|---|---|---|
| | Combination 4 | | | Combination 5 | | |
| | $f_{ac}$ | $f'_{ac}$ | $f_{bc}$ | $f_{ac}$ | $f'_{ac}$ | $f_{bc}$ |
| **A. Fixed Load** | | | | | | |
| 1. Self-weight Load | -11482 | -9196 | 14810 | -11482 | -9196 | 14810 |
| 2. Additional Dead Load | -1547 | -1239 | 1995 | -1547 | -1239 | 1995 |
| 3. Shrinkage | -945 | -411 | -804 | -945 | -411 | -804 |
| 4. Prestressing Force | 5695 | 2983 | -25502 | 5695 | 2983 | -25502 |
| **B. Transient Load** | | | | | | |
| 1. "D" Line Load | -5728 | -4588 | 7388 | - | - | - |
| 2. Braking Load | -116 | -93 | 150 | - | - | - |
| **C. Environment Load** | | | | | | |
| 1. Temperature | -1532 | -1990 | -912 | - | - | - |
| 2. Wind Load | -313 | -251 | 404 | - | - | - |
| 3. Earthquake Load | - | - | - | -1303 | -1044 | 1681 |
| **Stress Result** | **-15969** | **-14785** | **-2471** | **-9582** | **-8907** | **-7821** |

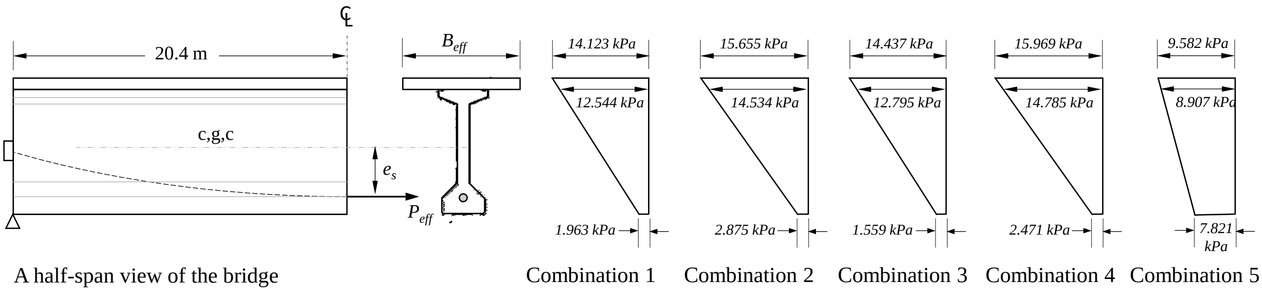


**Fig. 4** Stress diagram based on combination 1 – 5

Based on the loading combinations that have been summarized in Table 2 and Table 3 the results show that there is no tensile stress is found in any critical sections of the girder in all load combinations. The stress that occurs has fulfilled the design capacity, without any tensile stress occurring in the bridge. In the subsequent research, a verification process will be conducted to compare the obtained stress results with the stress analysis generated from numerical modelling.

## 4. Conclusion

In this study, our objective was to conduct stress analysis on PCI-Girder precast concrete segmental bridges based on SNI 1725:2016. 3 (three) Types of loads will be combined to obtain optimal conditions that may occur on the bridge. The first load is a Fixed load which includes the self-weight Load, additional dead load, load due to shrinkage or creep, and load due to prestressing forces. The second load is the transient action which includes the lane "D" lane load and the braking load. The third load is Environmental load which includes the influence of temperature, wind load, and earthquake, load. Through our analytical approach, we have found that the design of PCI-Girder precast concrete segmental bridges meets the safe design capacity according to SNI 1725:2016.

In conclusion, based on the loading combinations that have been summarized in Table 2 and Table 3, also the results in Fig. 4 show that no tensile stress is occurring in any critical sections of the girder in all load combinations. These findings have important implications for bridge design and construction practices involving PCI-Girder precast concrete segmental bridges. By ensuring the absence of tensile stress in critical sections, we can ensure the long-term structural reliability and performance of the bridges. The stress that occurs has fulfilled the design capacity, without any tensile stress occurring in the bridge. There is no need to install additional anchorages or external tendons at the joints between segments, but epoxy is still applied to form solid and monolithic properties of PCI Girder girders.

In future research, it is crucial to further verify the obtained stress analysis results by comparing them with stress analysis generated from numerical modelling. This step will provide increased confidence in the validity and accuracy of the analysis methods employed. Furthermore, research in this field should continue to advance toward the development of more sophisticated and efficient analysis methods, while considering the variability and uniqueness of PCI-Girder precast concrete segmental bridges. Further studies can also involve structural reliability analysis and dynamic simulations to evaluate the performance of these bridges.

JCEPD-ISSN: 2830-3628

**References**

[1] H. Jiang, Q. Cao, A. Liu, T. Wang, and Y. Qiu, "Flexural behavior of precast concrete segmental beams with hybrid tendons and dry joints," *Constr Build Mater*, vol. 110, pp. 1–7, 2016.

[2] H. Jiang, L. Chen, Z. J. Ma, and W. Feng, "Shear behavior of dry joints with castellated keys in precast concrete segmental bridges," *Journal of Bridge Engineering*, vol. 20, no. 2, p. 04014062, 2015.

[3] A. N. A. Hindi, M. E. KREGER, and J. E. Breen, "ENHANCING THE STRENGTH AND DUCTILITY OF POST-TENSIONED SEGMENTAL BOX-GIRDER BRIDGES. FINAL REPORT," 1991.

[4] H.-N. Cho, Y.-M. Choi, and B.-C. Sho, "Field load testing and reliability-based integrity assessment of segmental PC box girder bridges before opening to traffic," *Eng Struct*, vol. 20, no. 11, pp. 948–956, 1998.

[5] S. Saibabu, V. Srinivas, S. Sasmal, N. Lakshmanan, and N. R. Iyer, "Performance evaluation of dry and epoxy jointed segmental prestressed box girders under monotonic and cyclic loading," *Constr Build Mater*, vol. 38, pp. 931–940, 2013.

[6] H. Jiang, Q. Cao, A. Liu, T. Wang, and Y. Qiu, "Flexural behavior of precast concrete segmental beams with hybrid tendons and dry joints," *Constr Build Mater*, vol. 110, pp. 1–7, 2016.

[7] S. N. Indonesia and B. S. Nasional, "Pembebanan untuk jembatan," *SNI*, vol. 1725, p. 2016, 2016.

[8] N. D. Puspitasari and S. Munir, "Analysis of Shear Forces and Flaxural Moment at Joints in PCI-Girder Precast Concrete Segmental Bridge (Case Study: Konaweha River Bridge, Southeast Sulawesi)," 2022. [Online]. Available: www.ijisrt.com545

[9] E. Ketiga Jilid and H. Burns, "DESAIN STRUKTUR BETON PRATEGANG," 1982.

[10] E. G. Nawy, W. Hardani, and B. Suryoatmono, *Beton prategang: suatu pendekatan mendasar*. Erlangga, 2001.

[11] M. F. Granata, P. Margiotta, and M. Arici, "Simplified Procedure for Evaluating the Effects of Creep and Shrinkage on Prestressed Concrete Girder Bridges and the Application of European and North American Prediction Models," *Journal of Bridge Engineering*, vol. 18, no. 12, pp. 1281–1297, Dec. 2013, doi: 10.1061/(asce)be.1943-5592.0000483.

[12] P. J. Barr, A. M. Asce, ; B M Kukay, and M. W. Halling, "Comparison of Prestress Losses for a Prestress Concrete Bridge Made with High-Performance Concrete", doi: 10.1061/ASCE1084-0702200813:5468.

[13] W. Lin and T. Yoda, *Bridge engineering: classifications, design loading, and analysis methods*. Butterworth-Heinemann, 2017.

JCEPD-ISSN: 2830-3628